Rheology of Supercooled Se-Te Chain Liquids: Role of Te as an Interchain Cross-linker

[1]Bing Yuan, [2]Bruce Aitken, [1]Sabyasachi Sen*

[1]Department of Materials Science & Engineering, University of California at Davis,

Davis, CA 95616, USA

[2]Science & Technology Division, Corning Inc., Corning, NY 14831, USA

*Corresponding Author: Sabyasachi Sen (email: sbsen@ucdavis.edu)

Abstract

The shear relaxation behavior of supercooled Se_xTe_{100-x} ($70 \leq x \leq 95$) liquids are studied using oscillatory parallel plate rheometry. The difference in the relaxation timescales of the slow bond scission/renewal dynamics and the fast segmental chain motion that coexist in Se decreases monotonically with progressive addition of Te, until only one relaxation process can be identified in the $Se_{70}Te_{30}$ liquid. This evolution of the relaxation dynamics mimics the rheological behavior of Ge/As-Se liquids, when traditional chain crosslinkers such as Ge/As is added to Se. This finding suggests that the Te atoms serve as pseudo-crosslinkers via secondary bonding interactions between adjacent $[Se,Te]_n$ chains. This interchain interaction results in a lowering of the motional degrees of freedom of the constituent chains in Se_xTe_{100-x} liquids in the supercooled region. However, the compositional invariance of the superliquidus viscosity of these liquids suggests that the interchain interaction constraint can be lifted at high temperatures.

1. INTRODUCTION

Selenium (Se) and tellurium (Te) are isoelectronic chalcogens with strong structural similarities. The structure of stable crystalline polymorphs of Se and Te consist of polymeric $[Se]_n$ or $[Te]_n$ helical chains, where Se and Te atoms are twofold coordinated and form lattices with trigonal and hexagonal symmetry, respectively [1,2]. In addition, Se can also exist as a metatstable monoclinic allotrope that consists of Se_8 rings [1]. On the other hand, recent high-resolution ^{77}Se NMR spectroscopic results have shown that amorphous Se derived via melt-quenching consists practically solely of $[Se]_n$ chains, as no Se in the ring environment could be detected [3].

However, in spite of their structural similarities, Se and Te exhibit rather different glass forming abilities [4,5]. Se forms bulk glass rather easily upon quenching of the parent melt, while Te displays a strong tendency for crystallization upon supercooling and, therefore, forms glass only in the form of thin films. This behavior of Te is believed to result from strong secondary bonding interactions (SBI) between adjacent $[Te]_n$ chains. The SBIs between the neighboring Te atoms in adjacent chains are thought to result from the overlap between the Te 5p electron lone pair in one chain and the empty antibonding σ* orbital of Te in an adjacent chain, and such interactions can become as strong as the primary covalent Te-Te bonds within a chain [6]. These interactions involving delocalization of Te 5p electrons are also believed to be responsible for its higher metallicity compared to S or Se as well as the metallic character of liquid Te [6–10]. Another possible explanation for the metallic behavior of liquid Te is the shortening of $[Te]_n$ chains resulting from bond dissociation at high temperatures. This process can lead to an increased density of unpaired electrons associated with the Te atoms at the chains terminations and electron hopping between the short chain segments [11,12].

Although the crystalline structures of Se and Te share strong similarities, the coordination number of Te in the liquid phase has been debated for a long time. Previous studies based on neutron diffraction suggested Te to be present in both twofold and threefold coordination with an average coordination number of ~ 2.5 [13–16]. On the other hand, Silva and Cutler claimed on the basis of optical spectroscopic studies that Te exists in twofold coordination in liquid Se-Te alloys with up to 80% Te [11]. The bonding environment and the electronic interaction scenario for Te is clear in its crystalline state [6]. However, such understanding is still lacking for amorphous Te and tellurides, and could be crucial in building structure-property relationships in, for example, the Ge-Sb-Te phase change materials that are utilized in optical memory technology [17]. Binary Se-Te glasses constitute an interesting model system in this regard for the investigation of the SBI associated with Te atoms as glasses in this system are characterized by relatively simple blended copolymer $[Se,Te]_n$ chains of twofold coordinated Se and Te atoms [18–20]. Here we report the results of a rheological study of supercooled binary Se-Te liquids to demonstrate that the existence of such SBIs is clearly manifested in the viscoelastic relaxation behavior of these liquids. The proposed structural rationalization is found to be consistent with the compositional variation of the viscosity and the glass transition temperature T_g.

2. EXPERIMENTAL

2.1. Sample Preparation and physical characterization. Binary Se_xTe_{100-x} glasses with x = 95, 90, 80, 70 were prepared in ~14g batches from constituent elements using the conventional melt-quench method in evacuated fused quartz ampoules (6mm inner diameter). Mixtures of Se (Alfa Aesar, 99.999%) and Te (Alfa Aesar, 99.9999%) were taken in fused quartz ampoules that were evacuated (10^{-4} Torr) and flame sealed prior to loading into a rocking furnace. The ampoules were

heated to 873K over a period of 11 hours and subsequently held at this temperature for 12 hours to ensure homogeneity. The ampoules were then quenched in ice-water to obtain the glass samples.

All Se_xTe_{100-x} glasses were chemically analyzed using a Cameca SE-100 electron microprobe equipped with wavelength dispersive spectrometers to check for possible micron-scale phase separation. All glasses were found to be chemically homogeneous at the micron-scale and their compositions were within ±0.5at% of nominal. The glass transition temperature T_g was measured using a differential scanning calorimeter (Mettler-Toledo DSC1). Approximately 20 mg powdered glass sample was hermetically sealed in a 40 μL aluminum pan. Scans were taken in a flowing nitrogen environment with a heating rate of 20K /min. T_g was determined to within ± 2 °C as the onset of the glass transition.

2.2. Parallel Plate Rheometry. Small amplitude oscillatory shear (SAOS) rheological measurements on the Se_xTe_{100-x} supercooled liquids were carried out in a flowing Ar gas atmosphere using an Anton-Paar MCR92 parallel plate rheometer. The rheometer was operated under oscillatory mode with an 8 mm upper plate and a stationary lower plate with a gap of ~ 1 mm. Before the rheometry measurements, all samples were heated above their softening point, pressed and then trimmed to form a sandwich-like geometry between the plates. During each measurement, the samples were allowed to equilibrate at each temperature for 5 minutes, followed by the application of oscillatory strain with angular frequency ω varying between 1 and 600 rad/s within the linear viscoelastic range of the material and concomitantly the torque was measured to calculate the storage and the loss moduli G′ and G″ as a function of ω. Multiple measurements were carried out at multiple temperatures for each sample and master curves of G′(ω) and G"(ω) were constructed using time-temperature superposition (TTS). The viscosity master curves were

then calculated from the relation $\eta(\omega)=\frac{\sqrt{G'^2+G''^2}}{\omega}$. Details of the experimental setup and procedure can be found in a previous publication [21]. The Se_xTe_{100-x} glasses become increasingly susceptible to surface crystallization as the Te content increases. Therefore, fresh samples were used for rheological measurements at each temperature to avoid thermal cycling and each measurement was repeated on multiple samples to ensure reproducibility. The physical appearance of the samples was checked immediately after the end of each measurement, which indicated the lack of any discernible surface crystallization.

3. RESULTS AND DISCUSSION

The ω dependence of the storage modulus G' and the loss modulus G″ of the Se_xTe_{100-x} supercooled liquids is shown in Fig. 1 in the form of master curves after performing TTS to the raw data at a nearly iso-viscous (~ 10^7 Pa s) temperature. At low frequencies, in the terminal regime, all liquids display G' < G″ and a Maxwellian viscoelastic behavior with G' ~ ω^2 and G″~ ω. On the other hand, at the highest frequencies G' reaches a plateau which represents the high-frequency glassy shear modulus of the liquid, which is on the order of a few GPa. At this point the glass-forming liquids display a completely elastic behavior. The corresponding frequency-dependent viscosity $\eta(\omega) = \frac{\sqrt{G'^2+G''^2}}{\omega}$ data in Fig. 1 clearly demonstrate the expected rapid frequency-dependent drop in viscosity in this regime with increasing ω. More interestingly, G' displays another plateau region at intermediate frequencies, marking the first onset of frequency dependence of η (Fig. 1). This plateau is most prominent in pure Se and $Se_{95}Te_5$ liquids and still remains observable for the $Se_{90}Te_{10}$ liquid, while it is apparently absent in liquids with ≥20% Te (Fig. 1). Additionally, the low-frequency plateau modulus increases and the frequency separation

between the two plateaus decreases with progressive addition of Te. Recent studies have reported a similar compositional evolution of G′(ω) and G′′(ω) in As-Se and Ge-Se liquids as As or Ge is progressively added to Se. It was shown in these studies that the two plateaus in G'(ω) represent the existence of two relaxation processes with widely different timescales and relaxation moduli. The slow and the fast processes associated with the low- and high- frequency plateaus were found to correspond to Se-Se bond scission/renewal and Se chain segmental motion, respectively [22,23]. The fast process involving Se chain motion disappears on progressive addition of Ge or As to Se, due to the shortening of the chain segments as the chains are cross-linked to form a rigid three-dimensional network. It was found that Se chain segments shorter than ~ 3 to 5 Se atoms could not sustain the segmental motion as a pathway for shear relaxation [24].

Previous structural investigations using Raman and ^{77}Se nuclear magnetic resonance spectroscopy indicated that the Se_xTe_{100-x} binary glasses consist of $[Se,Te]_n$ chains [18–20] with nearly random distribution of Se and Te atoms in the chains. Therefore, it is reasonable to assume that, similar to Se, all Se_xTe_{100-x} liquids would also exhibit two relaxation processes: segmental chain motion and bond scission/renewal dynamics. However, as noted above, the evolution of the G'(ω) and G″(ω) spectra of these liquids with progressive addition of Te mimics that observed when known cross-linkers such as Ge or As are added to Se. The rheological data in Fig. 1 suggest that, while Se-rich compositions ($90 \leqslant x \leqslant 100$) have two distinct relaxation processes, further addition of Te results in a single relaxation process characteristic of network liquids.

Additional insight regarding the timescale distribution for these two relaxation processes can be gained from the corresponding relaxation spectrum H(τ), which can be calculated following Ninomiya and Ferry's method [25]:

$$H(\tau) = \frac{G'(a\omega) - G'(\omega/a)}{2\ln a} - \frac{a^2}{(a^2-1)^2}\frac{G'(a^2\omega) - G'(\omega/a^2) - 2G'(a\omega) + 2G'(\omega/a)}{2\ln a}\Bigg|_{1/\omega=\tau}$$

where *a* is the frequency increment on a logarithmic scale of the measurement. The H(τ) master curves for all compositions are shown in Fig. 2. The two peaks in H(τ) correspond to the most probable relaxation times for the two processes (Fig. 1). The presence of two relaxation processes can now be discerned even in the case of the $Se_{80}Te_{20}$ liquid (Fig. 2). It is evident from Fig. 2 that the slow process displays a rather narrow and symmetric Debye-type distribution of relaxation times, as would be intuitively expected for bond breaking dynamics, while the fast process is characterized by a much broader distribution of relaxation times. The relaxation strength of the slow process is significantly weaker, as bond scission/renewal events at any instant in the structure are expected to be few and spatially far between. On the other hand, the strength of the fast process is greater, and its broad time distribution is consistent with the widespread cooperative segmental motion of the chain moieties. Moreover, the temporal coupling between the two relaxation processes increases with increasing Te content, as the two peaks move closer to each other at a similar viscosity level until only one relaxation process can be seen in the highest Te containing $Se_{70}Te_{30}$ liquid (Fig. 2).

Simulation of these timescale distributions with Gaussian peaks (Fig. 2) indicates that the full-width-at-half-maximum (FWHM) of the distribution for the slow bond-breaking process is compositionally invariant (FWHM ~ 0.55 log units), except for pure Se, where it is narrower (FWHM ~ 0.35 log units). This result is possibly indicative of the fact that bond scission in Se-Te alloys involves 3 different bond types, namely Se-Se, Se-Te and Te-Te, as well as the secondary bonds involving Te atoms, while pure Se has only Se-Se bonds. On the other hand, the timescale

distribution for the fast process is the widest for pure Se (FWHM ~ 2 log units) and it decreases upon initial addition of Te (FWHM ~ 1.3 log units), beyond which it remains nearly constant until it decreases again in the $Se_{70}Te_{30}$ liquid, where only one relaxation process is observed (Fig. 2). When taken together, these results are consistent with a scenario where addition of Te to Se results in a strong SBI between chains, which effectively acts as pseudo-crosslinking (Fig. 3) with Te atoms serving as nodes that connect mobile selenium chain segments. Therefore, the SBI reduces the flexibility of the $[Se,Te]_n$ chains with progressive addition of Te atoms. Consequently, segmental chain motion becomes more difficult compared to that in pure Se and eventually culminates in bond scission. Thus, as evidenced in Figs 1 and 2, the two relaxation processes become increasingly temporally coupled with addition of Te, until only a single relaxation process is observed at the highest Te content. This pseudo cross-linking effect would be expected to result in a more rigid structure in binary Se_xTe_{100-x} glasses compared to that for pure Se. This hypothesis is indeed consistent with the observation that the T_g of Se_xTe_{100-x} glasses increases nearly linearly with Te content in this composition range (Fig. 4). Moreover, the increased rigidity of the structure is also evident in the temperature dependence of the viscosity of Se_xTe_{100-x} liquids determined in the present study as well as the viscosity data reported in the literature [26–29], which show a monotonic increase in isothermal viscosity with increasing Te content (Fig. 5). It may be noted here that the SBI between $[Se,Te]_n$ chains introduced by Te is likely weaker than the primary bonds introduced by conventional cross-linkers such as As/Ge, but significantly stronger than, for example, van der Waals interactions. In fact, the typical interatomic distance associated with the SBI is found to be somewhere intermediate between the characteristic values for covalent bonding and for van der Waals interactions. For example, typical Te-Te covalent bond length is ~ 2.7-2.8 Å while, the Te-Te SBI distance is ≥3.0 Å [6]. Therefore, the presence of the SBI in Se_xTe_{100-x}

glasses or liquids is not in any way indicative of an increased coordination number of Te atoms. Consequently, unlike the network formed with As/Ge-Se, the chain elements are retained in Se-Te Therefore, the SBI-related constraints will likely be lifted at high temperature and the dynamical behavior of $[Se,Te]_n$ chains would become quite similar to those characteristic of $[Se]_n$ chains. This scenario is in agreement with the high-temperature viscosity data for Se_xTe_{100-x} liquids, which show compositional invariance over a relatively wide range of viscosity in the superliquidus region (Fig. 5).

Finally, the relative coupling of the fast segmental chain motion and the slow bond scission/renewal dynamics to viscous flow can be estimated using the Maxwell relation according to which the contribution to the viscosity η from the slow process is given by $\eta_s = G_s\tau_s$ and that from the fast process is given by $\eta_f = (G_f - G_s)\tau_f \approx G_f\tau_f$[30]. The G and τ in these equations are the plateau shear moduli, and the relaxation time corresponding to the specific relaxation process, respectively. The $Se_{95}Te_5$ supercooled liquid is chosen for this purpose since the rheological data for this composition allow for direct determination of τ_s and τ_f at multiple temperatures from the locations of the onset of frequency dependence of $\eta(\omega)$, and G_s and G_f are estimated from Fig. 1 to be ~ 10^6 Pa and 10^9 Pa, respectively. The η_s and η_f are compared to the experimental $\eta_{exp.}$ for the $Se_{95}Te_5$ supercooled liquid in Fig. 6. It is clear from this comparison that both relaxation processes are coupled to viscous flow in their respective temperature ranges. This result is likely indicative of a mechanistic connection between the two dynamical processes in spite of their widely separated timescales. Although the exact nature of this connection remains unclear at this stage, it is tempting to speculate that the rapid segmental motion of the $[Se,Te]_n$ chains leads every so often to a locally highly strained state such that the chain can recover from it only via the breaking of a

Se/Te-Se/Te bond. This hypothesis could be tested in future studies using molecular dynamics simulation.

4. CONCLUSIONS

Chalcogens such as S and Se are typically characterized by twofold coordination in their elemental form as well as in a wide variety of crystalline and amorphous chalcogenide compounds. However, the bonding behavior of the heavier chalcogen Te remains controversial as, compared to the analogous sulfides and selenides, the increased metallicity of Te in its elemental form and in tellurides is believed to result from its strong SBI. It is shown in the present study that this SBI is manifested in the rheological behavior of Se_xTe_{100-x} supercooled liquids containing copolymeric $[Se,Te]_n$ chains. Our rheological measurements presented demonstrate that the timescales of the fast and slow relaxation processes in Se_xTe_{100-x} liquids with high Se content ($80 \leqslant x \leqslant 100$), which correspond to segmental chain motion and bond scission/renewal events, respectively, become increasingly coupled until only one relaxation process is observed for the $Se_{70}Te_{30}$ liquid. This gradual transition in the dynamical behavior is quite similar that displayed by Ge/As-Se liquids with increasing relative concentration of the conventional crosslinkers, namely Ge and As. When taken together, these results suggest that the SBI of Te results in a sufficiently strong interchain interaction in the Se_xTe_{100-x} liquids, such that Te atoms act as nodal points in the $[Se,Te]_n$ chains, imparting rigidity and, consequently, Te acts as a pseudo-crosslinker. This scenario is shown to be consistent with the compositional variation of T_g of these liquids and their isothermal viscosity in the supercooled regime. Moreover, the compositional invariance of viscosity at superliquidus temperatures suggests that the constraints imposed by the SBI between the $[Se,Te]_n$ chains are eventually overcome with increasing temperature. Viscosity contributions of the fast

and slow relaxation processes are estimated in the $Se_{95}Te_5$ supercooled liquid using the Maxwell relation. Both processes are shown to be closely related to viscosity in their respective temperature ranges, which might indicate a mechanistic coupling between them.

ACKNOWLEDGMENTS

This study is supported by the National Science Foundation Grant NSF-DMR 1855176.

REFERENCES

[1] G. Lucovsky, A. Mooradian, W. Taylor, G.B. Wright, R.C. Keezer, Identification of the fundamental vibrational modes of trigonal, α-monoclinic and amorphous selenium, Solid State Commun. 5 (1967) 113–117.

[2] E. Grison, Studies on tellurium-selenium alloys, J. Chem. Phys. 19 (1951) 1109–1113.

[3] M. Marple, J. Badger, I. Hung, Z. Gan, K. Kovnir, S. Sen, Structure of Amorphous Selenium by 2D ^{77}Se NMR Spectroscopy: An End to the Dilemma of Chain versus Ring, Angew. Chemie. 129 (2017) 9909–9913.

[4] A. Zakery, S.R. Elliott, Optical properties and applications of chalcogenide glasses: A review, J. Non. Cryst. Solids. 330 (2003) 1–12.

[5] M. Popescu, Non-Crystalline Chalcogenides, Kluwer Academic Publishers, 2002.

[6] T. Chivers, R.S. Laitinen, Tellurium: A maverick among the chalcogens, Chem. Soc. Rev. (2015) 1725–1739.

[7] S. Yi, Z. Zhu, X. Cai, Y. Jia, J.H. Cho, The Nature of Bonding in Bulk Tellurium Composed of One-Dimensional Helical Chains, Inorg. Chem. 57 (2018) 5083–5088.

[8] H. Endo, Structural and electronic properties of liquid tellurium, J. Non. Cryst. Solids. 156–159 (1993) 667–674.

[9] S. Tamaki, Phase transition in liquids, Phase Transitions. 66 (1998) 167–257.

[10] Y. Tsuchiya, The anomalous negative thermal expansion and the compressibility maximum of molten Ge-Te alloys, J. Phys. Soc. Japan. (1991) 227–234.

[11] L.A. Silva, M. Culter, Optical properties of liquid Se-Te alloys, Phys. Rev. B. 42 (1990) 7103.

[12] M. Misawa, A short-chain model for local structure in liquid tellurium, J. Phys. Condens. Matter. 4 (1992) 9491–9500.

[13] B. Cabane, J. Friedel, Local order in liquid tellurium, J. Phys. 32 (1971) 73.

[14] G. Tourand, B. Cabane, M. Breuil, Structure of liquid tellurium, J. Non. Cryst. Solids. 8–10 (1972) 676–686.

[15] A. Menelle, R. Bellissent, A.M. Flank, Short range order in liquid Se-Te system by neutron scattering, Phys. B Condens. Matter. 157 (1989) 174–176.

[16] M.E. Welland, M. Gay, J.E. Enderby, Physics of disordered systems, Plenum Press, New York, 1985.

[17] M. Wuttig, N. Yamada, Phase-change materials for rewriteable data storage, Nat. Mater. 6 (2007) 824.

[18] K. Itoh, Structure of Se-Te glasses studied using neutron, X-ray diffraction and reverse Monte Carlo modelling, J. Solid State Chem. 246 (2017) 372–378.

[19] B. Bureau, C. Boussard-plèdel, M. Lefloch, J. Troles, J. Lucas, D. Rennes, D. Beaulieu, Selenium-Tellurium Sequences in Binary Glasses as Depicted by ^{77}Se and ^{125}Te NMR, 109 (2005) 6130–6135.

[20] A. Tverjanovich, A. Cuisset, D. Fontanari, E. Bychkov, Structure of Se-Te glasses by Raman spectroscopy and DFT modeling, J. Am. Ceram. Soc. 101 (2018) 5188–5197.

[21] S. Sen, W. Zhu, B.G. Aitken, Behavior of a supercooled chalcogenide liquid in the non-Newtonian regime under steady vs. oscillatory shear, J. Chem. Phys. 147 (2017) 034503.

[22] W. Zhu, B.G. Aitken, S. Sen, Observation of a Dynamical Crossover in the Shear Relaxation Processes in Supercooled Selenium Near the Glass Transition, J. Chem. Phys. 150 (2019) 094502.

[23] W. Zhu, I. Hung, Z. Gan, B. Aitken, S. Sen, Dynamical process related to viscous flow in a supercooled arsenic selenide glassforming liquid: Results from high-temperature ^{77}Se NMR Spectroscopy, J. Non. Cryst. Solids. (2019). (Accepted)

[24] S. Sen, Y. Xia, W. Zhu, M. Lockhart, B. Aitken, Nature of the floppy-to-rigid transition in chalcogenide glass-forming liquids, J. Chem. Phys. 150 (2019) 144509.

[25] J.D. Ferry, Viscoelastic properties of polymers, John Wiley & Sons, 1980.

[26] P. Koštál, J. Málek, Viscosity of selenium melt, J. Non. Cryst. Solids. 356 (2010) 2803–2806.

[27] P. Koštál, J. Málek, Viscosity of Se-Te glass-forming system, Pure Appl. Chem. 87 (2015) 239–247.

[28] J.C. Perron, J. Rabit, J.F. Rialland, Impurity dependence of the viscosity of liquid selenium, Philos. Mag. B Phys. Condens. Matter; Stat. Mech. Electron. Opt. Magn. Prop. 46 (1982) 321–330.

[29] J. Barták, P. Koštál, D. Valdés, J. Málek, T. Wieduwilt, J. Kobelke, M.A. Schmidt, Analysis of viscosity data in As_2Se_3, Se and $Se_{95}Te_5$ chalcogenide melts using the pressure assisted melt filling technique, J. Non. Cryst. Solids. 511 (2019) 100–108.

[30] T. Scopigno, S.N. Yannopoulos, F. Scarponi, K.S. Andrikopoulos, D. Fioretto, G. Ruocco, Origin of the λ transition in liquid sulfur, Phys. Rev. Lett. 99 (2007) 025701.

Figure Captions

Figure 1. Master curves of the frequency dependence of storage modulus G′ (squares), loss modulus G″ (circles), and viscosity (triangles) of Se_xTe_{100-x} liquids. The composition and the reference temperatures for TTS are listed in the inset of each panel. Data for pure Se are shown for comparison and are taken from Zhu *et al* [22].

Figure 2. Relaxation spectra H(τ) of Se_xTe_{100-x} liquids. Filled squares represent the experimental data. Open squares and circles are Gaussian components fitted to the fast and slow process, respectively. Solid lines represent the sum of the two components i.e. total fit to the experimental data. Data for the H(τ) spectrum of pure Se is taken from Zhu *et al* [22].

Figure 3. Cartoon showing SBI (dashed red line) between Te atoms in adjacent $[Se,Te]_n$ chain segments in the binary Se-Te system.

Figure 4. Glass transition temperature T_g of binary Se_xTe_{100-x} glasses.

Figure 5. Temperature dependence of viscosity of pure Se and binary Se-Te liquids as reported in the literature [26–29]. Inset shows the comparison between data collected in the present study (filled symbols) and literature data (open symbols) in the supercooled region.

Figure 6. Viscosity contributions from the slow process η_s (filled pentagons) and from the fast process $\eta_f = G_f\tau_f$ (filled triangles) for supercooled $Se_{95}Te_5$ liquid are compared to experimentally measured viscosity from the present study (filled squares) and from literature (open circles) [27].

Fig. 1

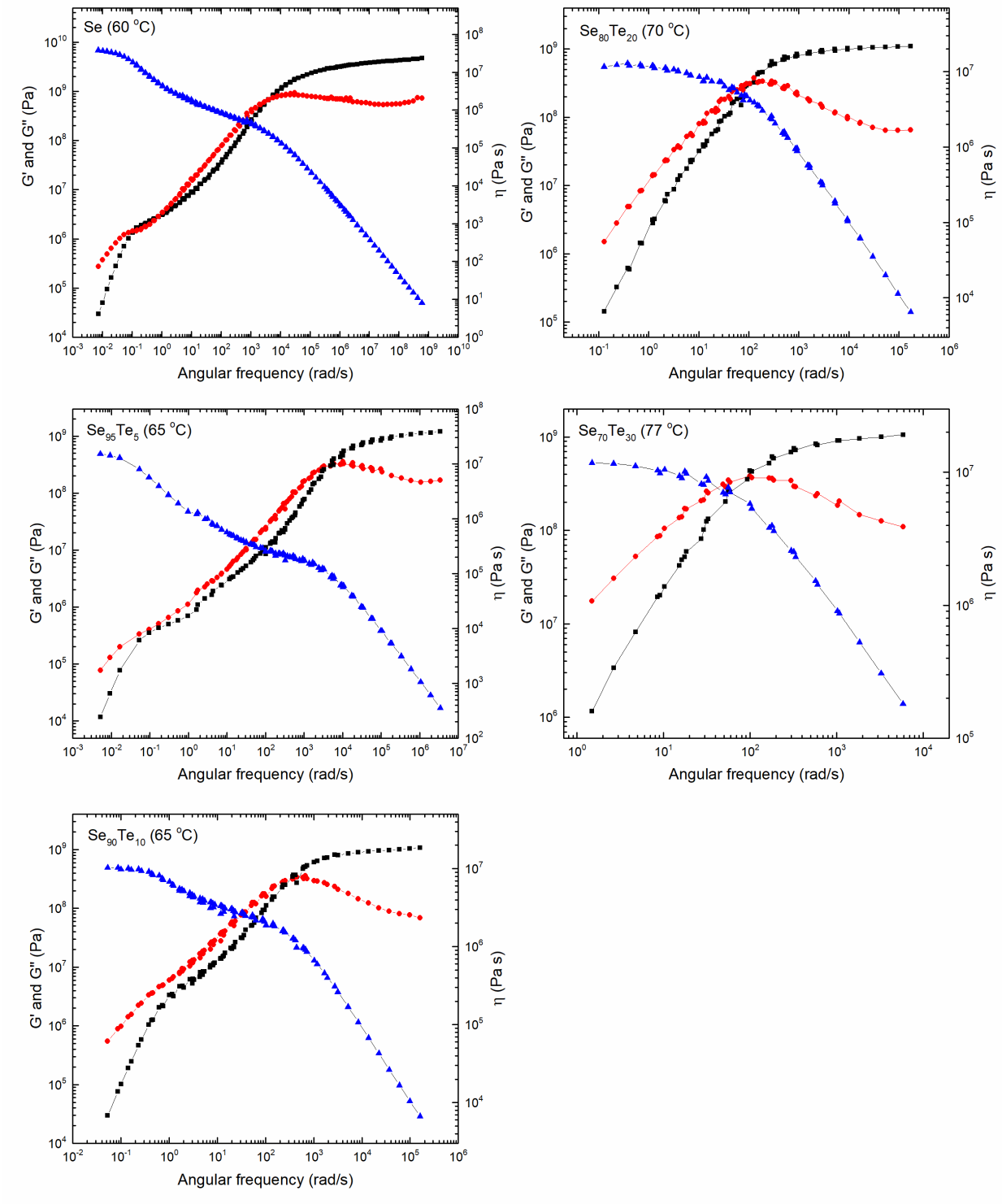
Se (60 °C)
Se80Te20 (70 °C)
Se95Te5 (65 °C)
Se70Te30 (77 °C)
Se90Te10 (65 °C)
G' and G'' (Pa)
η (Pa s)
Angular frequency (rad/s)

Fig. 2

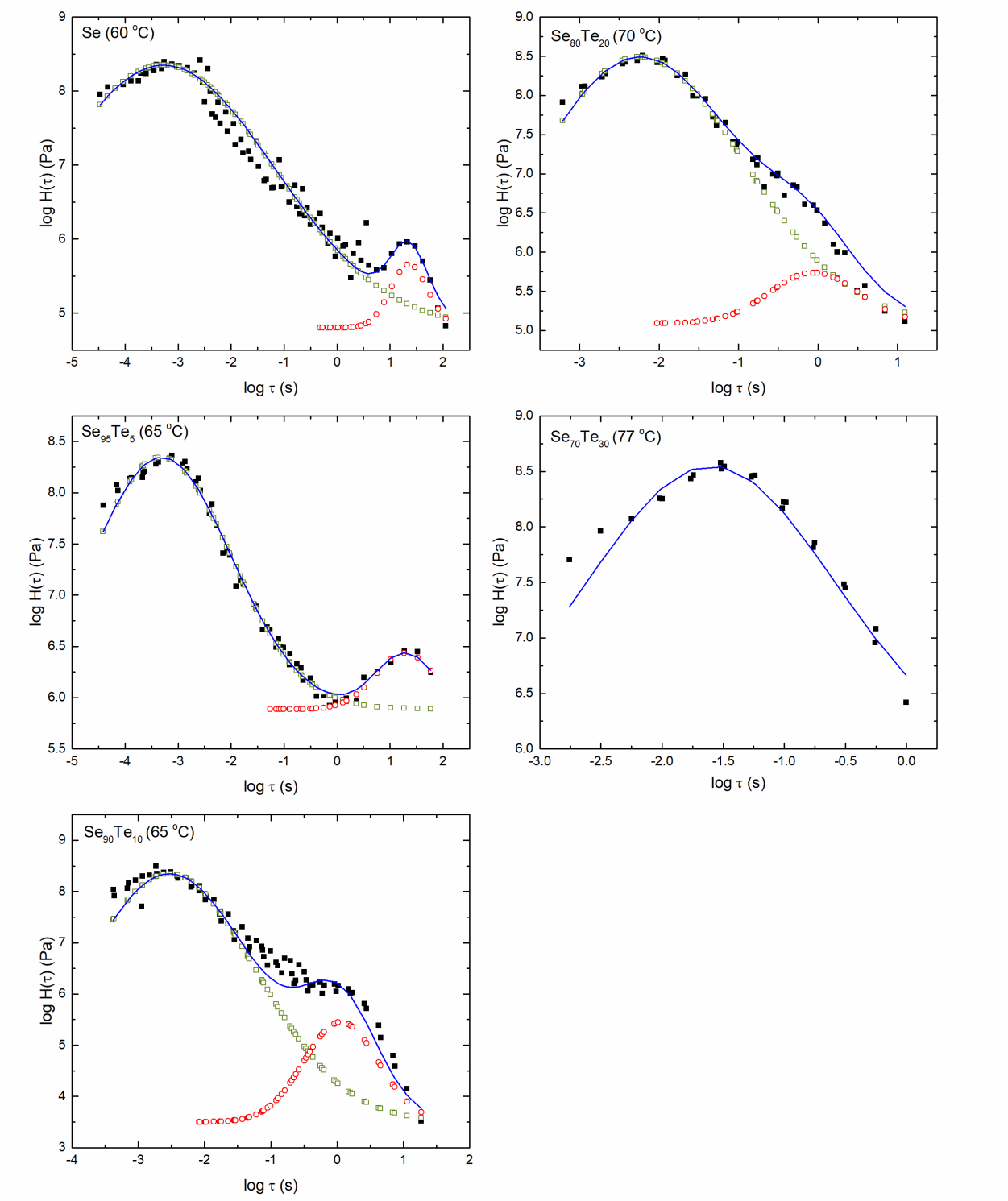
Se (60 °C)
Se80Te20 (70 °C)
Se95Te5 (65 °C)
Se70Te30 (77 °C)
Se90Te10 (65 °C)
log H(τ) (Pa)
log τ (s)

Fig. 3

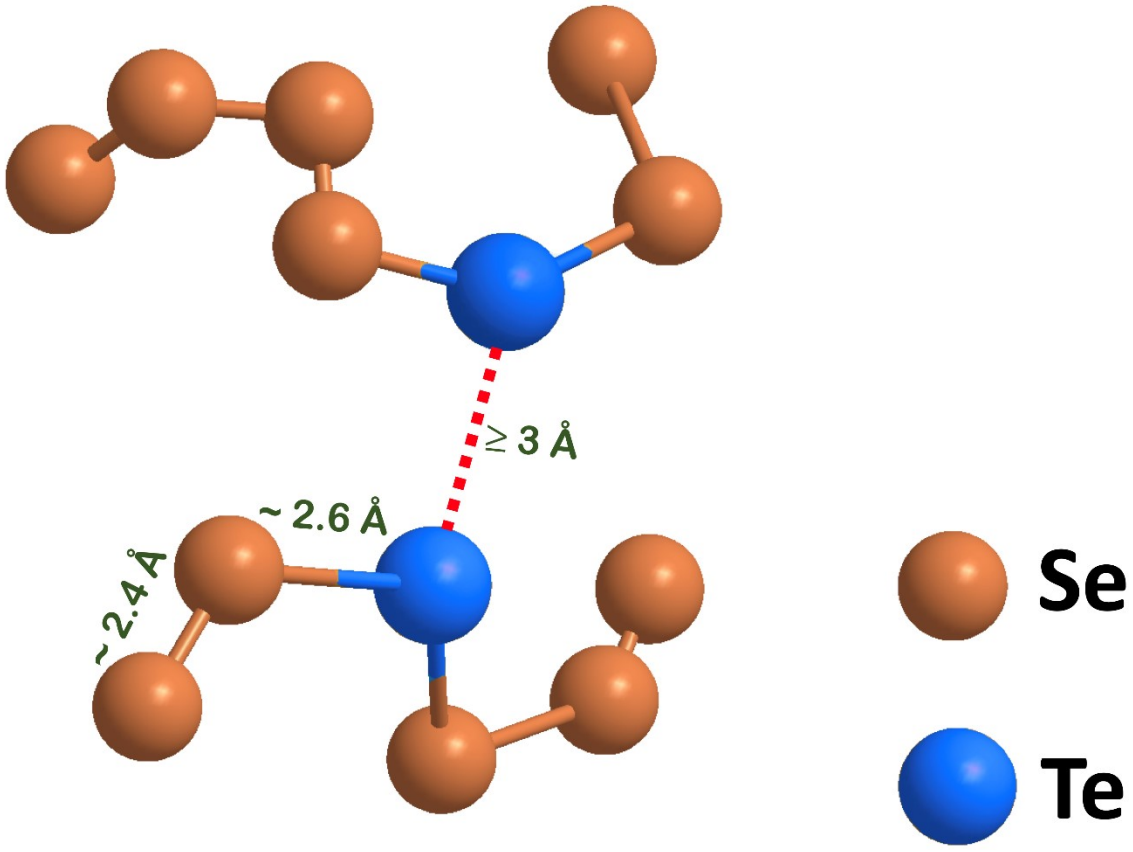

Fig. 4

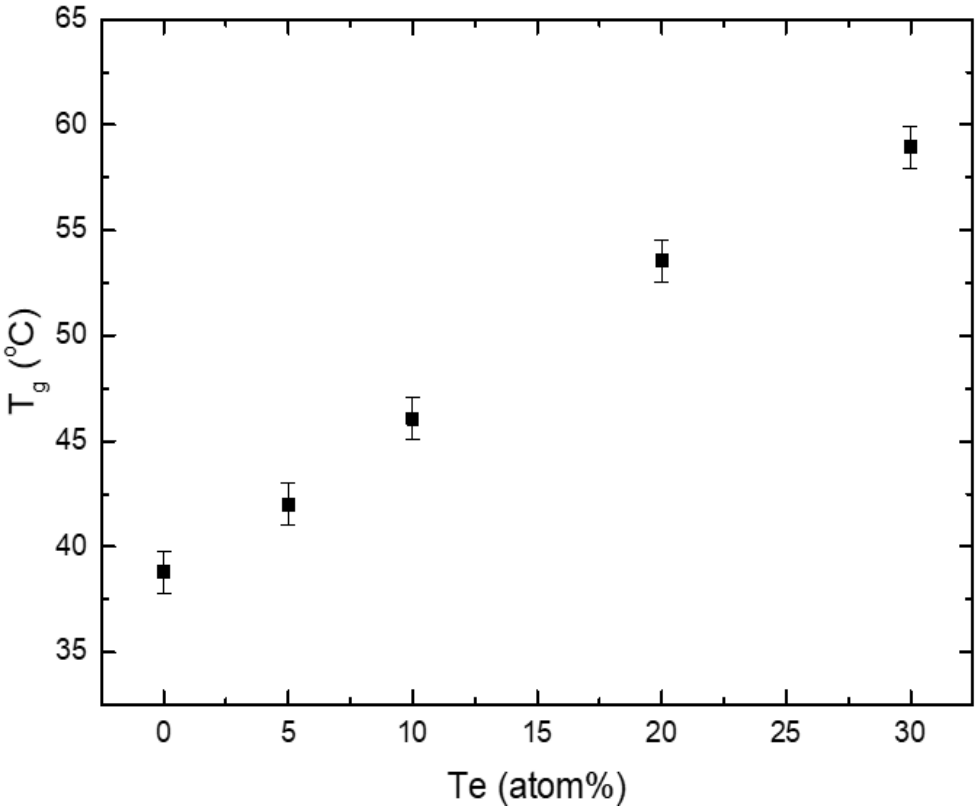

Fig. 5

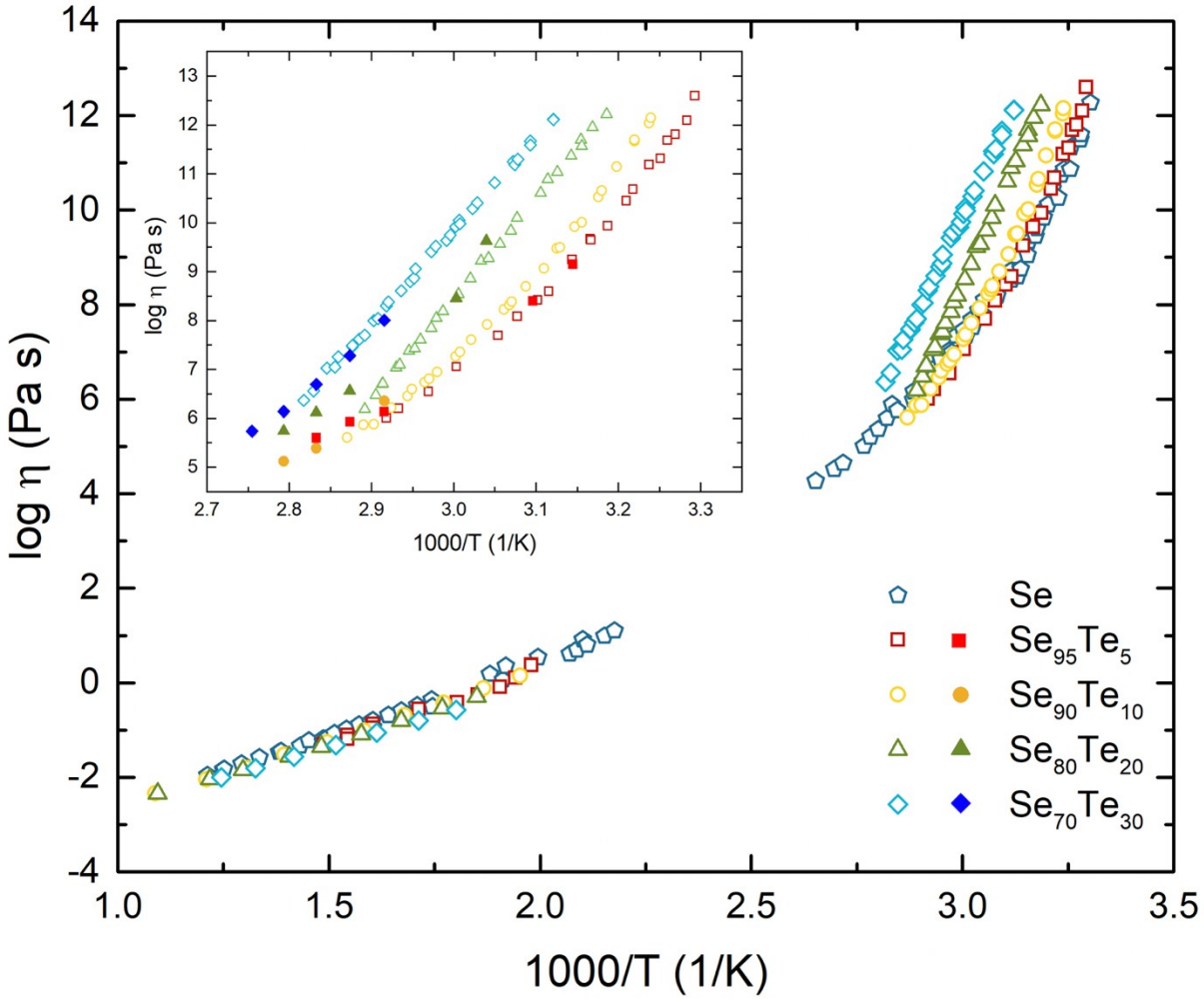

Fig. 6

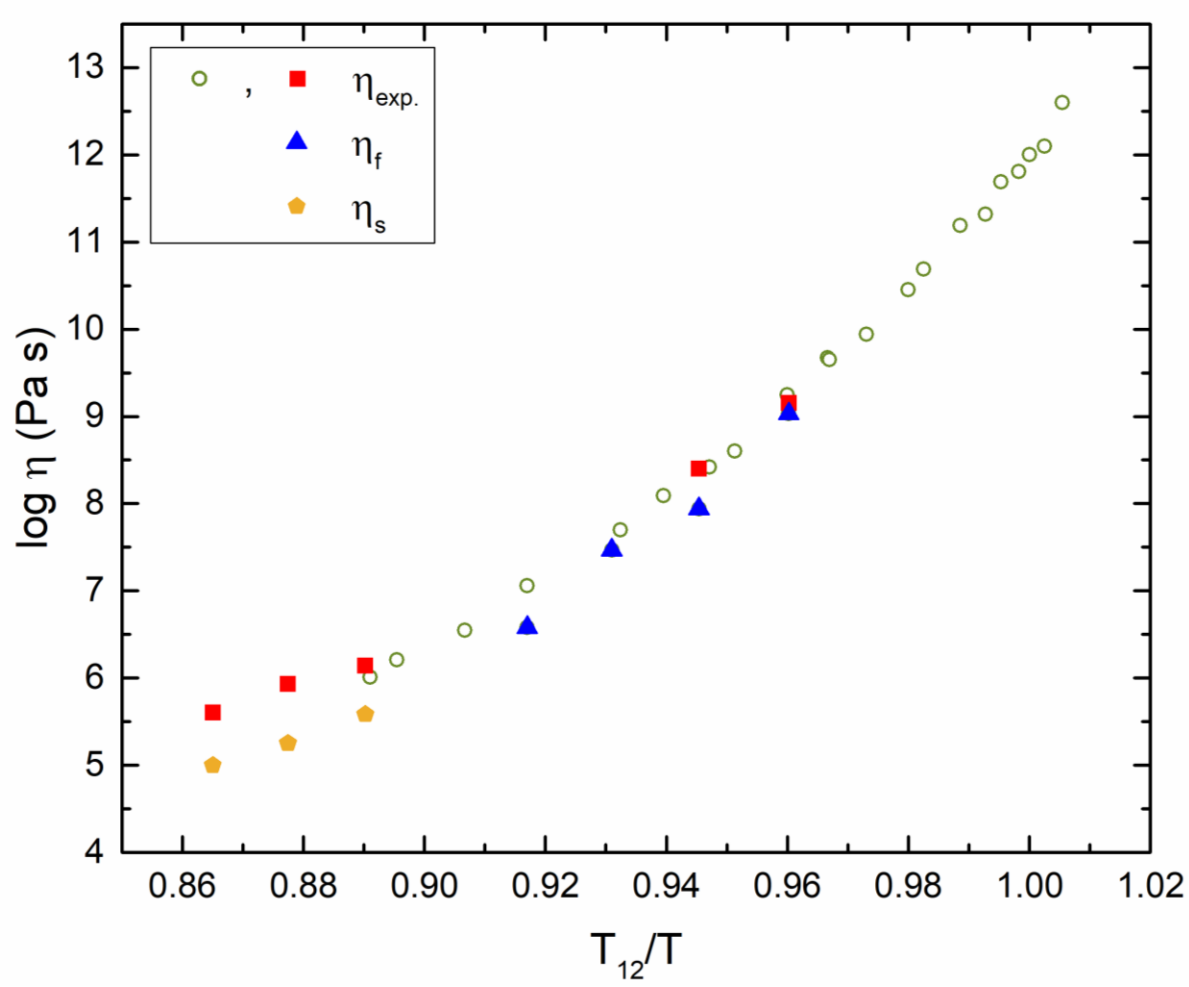
log η (Pa s)
T12/T
ηexp.
ηf
ηs
13
12
11
10
9
8
7
6
5
4
0.86
0.88
0.90
0.92
0.94
0.96
0.98
1.00
1.02